MANIPAL UNIVERSITY JAIPUR
(University under Section 2(f) of the UGC Act)

Effect of a Continued-Fraction Potential on Binary Star System Transport via Invariant Manifolds

Bhupendra Jangid, Ashok Kumar Pal
Department of Mathematics and Statistics
Manipal University Jaipur, Jaipur, Rajasthan, India 303007

Abstract

The Central Parsec of the Galaxy hosts numerous binary and multiple star systems immersed in strong radiation fields and embedded non-spherical dusty structures. This study models the local stellar dynamics around a binary star system using a modified Circular Restricted Three-Body Problem (CRTBP). The binary is represented by a massive radiating primary and a non-spherical secondary star whose gravitational asymmetry, arising from tidal distortion, extended envelopes, or circumstellar material, is modeled using a continued-fractional potential. Within this framework, we examine the phase-space structure by computing Lyapunov periodic orbits under the influence of the continued-fractional potential and propagating their invariant manifolds to identify heteroclinic connections between the dynamical regions of the two stars. These pathways act as natural low-energy transport channels, offering insight into the migration of matter and small bodies in the dense Galactic Center environment.

Model Formulation

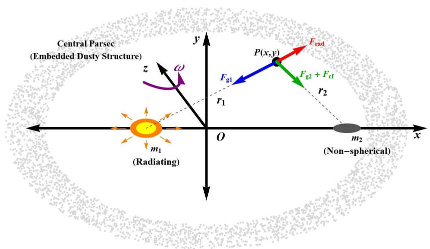

Figure 1. Schematic of the modified CR3BP in the Galactic Center environment.

Modified Effective Potential Ω^*:

$$\Omega^* = \frac{1}{2}(x^2+y^2) + \frac{r_p\,(1-\mu)}{r_1} + \frac{\mu\, r_2}{{r_2}^2+\epsilon} + \frac{M_d}{\sqrt{r^2+T^2}}$$

Mean Motion (ω):

$$\omega^2 = \frac{1-\epsilon}{(1+\epsilon)^2} + 2\frac{M_d r_0}{(r_0^2+T^2)^{\frac{3}{2}}}$$

Equations of Motion:

$$\ddot{x} - 2\omega\dot{y} = \frac{\partial\Omega^*}{\partial x}, \qquad \ddot{y} + 2\omega\dot{x} = \frac{\partial\Omega^*}{\partial y}$$

Lyapunov Orbits

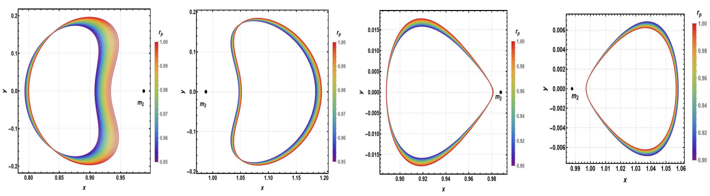

(a) Around L_1 (b) Around L_2 (c) Around L_1' (d) Around L_2'

Figure 2: Comparative analysis of the Lyapunov periodic orbits around the collinear points L_1, L_2, L_1' and L_2' for different values of the r_p.

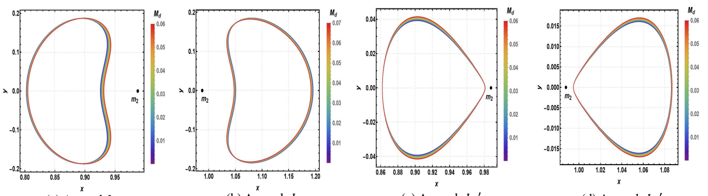

(a) Around L_1 (b) Around L_2 (c) Around L_1' (d) Around L_2'

Figure 3: Comparative analysis of the Lyapunov periodic orbits around the collinear points L_1, L_2, L_1' and L_2' for different values of the M_d.

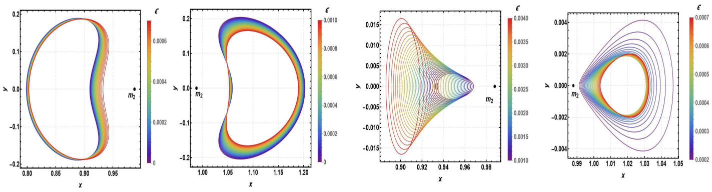

(a) Around L_1 (b) Around L_2 (c) Around L_1' (d) Around L_2'

Figure 4: Comparative analysis of the Lyapunov periodic orbits around the collinear points L_1, L_2, L_1' and L_2' for different values of the ϵ.

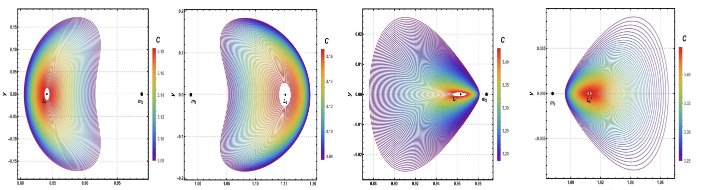

(a) Around L_1 (b) Around L_2 (c) Around L_1' (d) Around L_2'

Figure 5: Family of Lyapunov periodic orbits around the collinear points L_1, L_2, L_1' and L_2' for a system with mass parameter ($\mu = 0.01215$).

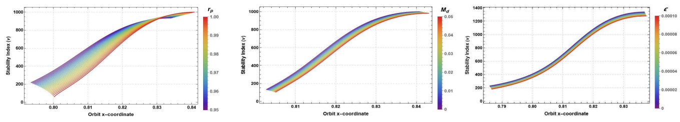

(a) (b) (c)

Figure 6: Variation of the stability index ν with perturbing parameters for Lyapunov orbits around the collinear point L_1.

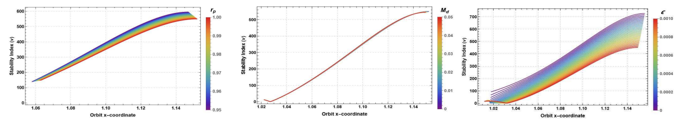

(a) (b) (c)

Figure 7: Variation of the stability index ν with perturbing parameters for Lyapunov orbits around the collinear point L_2.

Invariant Manifolds

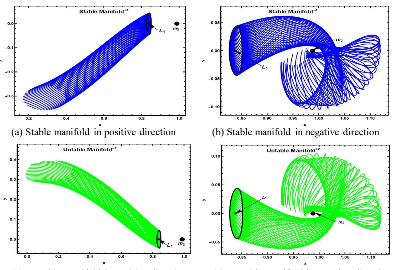

(a) Stable manifold in positive direction (b) Stable manifold in negative direction (c) Unstable manifold in positive direction (d) Unstable manifold in negative direction

Figure 8: Invariant manifolds of Lyapunov orbits around L_1 at $\epsilon = 0.0002$ for mass parameter ($\mu = 0.01215$).

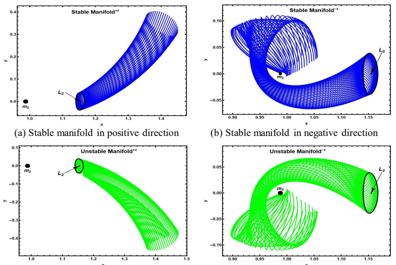

(a) Stable manifold in positive direction (b) Stable manifold in negative direction (c) Unstable manifold in positive direction (d) Unstable manifold in negative direction

Figure 9: Invariant manifolds of Lyapunov orbits around L_2 at $\epsilon = 0.0002$ for mass parameter ($\mu = 0.01215$).

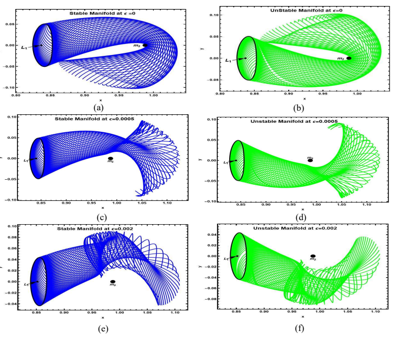

Figure 10: Invariant manifold of Lyapunov orbits around L_1 at $\epsilon = 0, \epsilon = 0.0005$ and $\epsilon = 0.002$ for mass parameter ($\mu = 0.01215$).

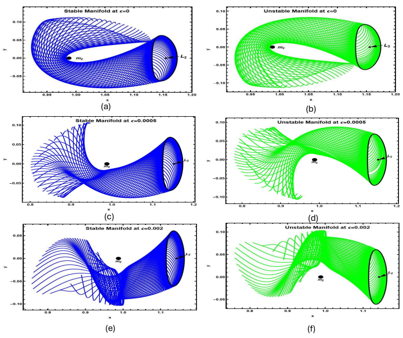

Figure 11: Invariant manifold of Lyapunov orbits around L_2 at $\epsilon = 0, \epsilon = 0.0005$ and $\epsilon = 0.002$ for mass parameter ($\mu = 0.01215$).

Homoclinic and Heteroclinic connections

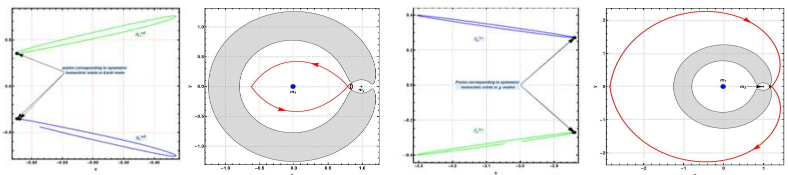

(a) The first Poincare cut of stable and unstable manifold tubs with y = 0 for L_1 Lyapunov orbit.
(b) A symmetric (1,1)-homoclinic orbit in the E realm
(c) The first Poincare cut of stable and unstable manifold tubs with y = 0 for L_2 Lyapunov orbit.
(d) A symmetric (2,2)-homoclinic orbit in the χ realm

Figure 12: The Poincaré cuts and homoclinic orbits with mass parameter ($\mu = 0.01215$) at $\epsilon = 2\times 10^{-6}$.

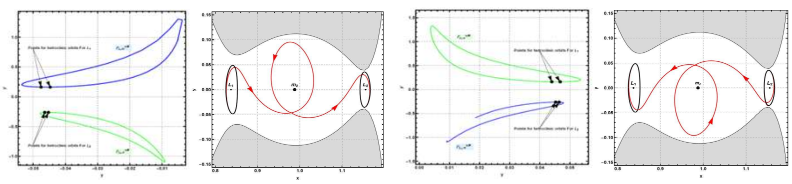

(a) The first Poincare cut of stable and unstable manifold tubs with P_3 for the L_1 and L_2 Lyapunov orbits
(b) A symmetric (1,2)-heteroclinic orbit in the M realm
(c) The first Poincare cut of stable and unstable manifold tubs with P_2 for the L_1 and L_2 Lyapunov orbits
(d) A symmetric (1,2) −heteroclinic orbit in the M realm

Figure 13: The Poincare cuts and heteroclinic orbits with mass parameter ($\mu = 0.01215$) at $\epsilon = 2\times 10^{-6}$.

Conclusion

In this study, we investigated the motion of an infinitesimal body in the neck region and demonstrated the existence of both transit and non-transit orbits for a fixed energy surface. Lyapunov orbits and their families were computed for the mass parameter ($\mu = 0.01215$) using the differential correction method. The results show that the fractional parameter ϵ strongly influences the amplitude and geometry of the Lyapunov orbits. For the mass parameter $\mu = 0.01215$, the amplitudes around the L_1 and L_2 points decrease as ϵ increases. Invariant manifolds associated with these orbits were also constructed, representing natural transport trajectories in space. Their intersections with Poincaré sections reveal possible transfer pathways within the system. Furthermore, homoclinic and heteroclinic orbits were obtained, connecting different dynamical regions and enabling efficient halo-to-halo transfers. Overall, the study highlights the important role of ϵ in orbit dynamics, stability, and transfer trajectory design.

ACKNOWLEDGEMENT

The authors acknowledge the University Grants Commission (UGC), India, for providing the Senior Research Fellowship (SRF). We sincerely thank Manipal University Jaipur for the research facilities. Furthermore, we are grateful to the Anusandhan National Research Foundation (ANRF), Government of India, and the International Astronomical Union (IAU) for the financial support enabling participation in the IAU Symposium.

REFERENCES

1. Howell, K.C., Beckman, M., Patterson, C. and Folta, D., 2006. Representations of invariant manifolds for applications in three-body systems. *The Journal of the Astronautical Sciences*, *54*(1), pp.69-93.
2. Gómez, G., Marcote, M. and Mondelo, J.M., 2005. The invariant manifold structure of the spatial Hill's problem. *Dynamical Systems*, *20*(1), pp.115-147.
3. Llibre, J., Martínez, R. and Simó, C., 1985. Tranversality of the invariant manifolds associated to the Lyapunov family of periodic orbits near L2 in the restricted three-body problem. *Journal of Differential Equations*, *58*(1), pp.104-156.
4. Abouelmagd, E.I., 2018. Periodic solution of the two–body problem by KB averaging method within frame of the modified newtonian potential. *The Journal of the Astronautical Sciences*, *65*(3), pp.291-306.